Title:

Development and Evaluation of Curcumin Phytosomes Using Sunflower Lecithin via Rotary Evaporation: A Strategy to Enhance Bioavailability.

KHOPADE NIKHIL MARUTI^{1*}, KAKASAHEB J. KORE², SUCHETA DILIP BHISE², MADHURI S KESKAR² & RAJKUMAR V. SHETE³

¹Rajgad Dnyanpeeth's College of Pharmacy Bhor, Savitribai Phule Pune University, Pune, Maharashtra,

²Department of pharmaceutics.Rajgad Dnyanpeeth's College of Pharmacy Bhor,Pune

³Department of Pharmacology. Rajgad Dnyanpeeth's College of Pharmacy, Bhor, Pune 412206. India.

Abstract

Curcumin, a bioactive polyphenol with demonstrated antioxidant, anti-inflammatory, and anticancer properties, faces significant clinical limitations due to poor aqueous solubility (<1 $\mu g/mL$) and low oral bioavailability (<1%). This study developed curcumin phytosomes using sunflower lecithin and the rotary evaporation method to address these challenges. The optimized formulation (curcumin:lecithin molar ratio 1:5) exhibited a high entrapment efficiency (84.69 \pm 0.51%), yield (88.12 \pm 2.5%), and particle size (356.48 \pm 3.7 nm) with a zeta potential of -45.22 mV, indicating colloidal stability. In vitro release studies demonstrated sustained drug release (90.1% over 12 hours), following the Korsmeyer-Peppas model. Stability tests under refrigerated conditions (4°C) retained >83% drug content for 3 months. These results validate rotary evaporation as a scalable method for producing sunflower lecithin-based phytosomes, offering a promising solution to enhance curcumin's therapeutic potential.

Keywords: Curcumin, phytosomes, sunflower lecithin, rotary evaporation, bioavailability.

1. Introduction

Curcumin, the principal curcuminoid in turmeric (Curcuma longa), has garnered attention for its broad-spectrum pharmacological activities, including anticancer, anti-inflammatory, and neuroprotective effects. Despite its therapeutic promise, curcumin's clinical utility is hindered by poor solubility, rapid metabolism, and low bioavailability. Conventional formulations often fail

to achieve therapeutic plasma concentrations, necessitating advanced delivery systems.(1-3)

Phytosomes, phospholipid-based nanocarriers, improve the bioavailability of hydrophobic compounds by forming lipid-compatible complexes. While soy lecithin is traditionally used, sunflower lecithin offers advantages such as allergen-free composition, higher phosphatidylcholine content (≥70%), and oxidative stability. This study employs rotary evaporation-a solvent-free, scalable technique-to develop curcumin phytosomes, addressing gaps in existing methodologies.(3-5)

2. Materials and Methods

2.1 Materials

Curcumin (≥95% purity, Sahydri Natural & phytochemist , India) and sunflower lecithin (phosphatidylcholine content ≥70%, Intare direct trading company Naturals, India) were used as the primary components. Ethanol (HPLC grade, Merck, Germany) and dichloromethane (analytical grade, Fisher Scientific, India) served as solvents for dissolving the drug and lipid. Phosphate buffer saline (PBS, pH 6.8) was prepared using sodium phosphate dibasic (Na₂HPO₄) and potassium phosphate monobasic (KH₂PO₄) (Sigma-Aldrich, India). Ultrapure water (Milli-Q Advantage A10, Millipore, India) was used for hydration and dilution.(6)

2.2 Preparation of Curcumin Phytosomes

The phytosomes were prepared using a rotary evaporation method adapted from with modifications for sunflower lecithin. Curcumin and sunflower lecithin were weighed in molar ratios ranging from 1:1 to 1:5 and dissolved in a 3:1 (v/v) ethanol-dichloromethane solvent system. The mixture was stirred magnetically at 500 rpm and 40°C for 30 minutes to ensure complete dissolution. The homogeneous solution was transferred to a rotary evaporator

(Buchi Rotavapor R-300, Switzerland) and evaporated under reduced pressure (200 mbar) at 60°C with a rotation speed of 100 rpm for 20–30 minutes, forming a thin lipid-drug film on the flask walls. (7) The film was hydrated with 10 mL of PBS (pH 6.8) at 60°C for 1 hour to facilitate vesicle formation. The resultant dispersion was probe-sonicated (Sonics Vibra-Cell VCX 750, USA) at 60% amplitude for 5 cycles (30 seconds pulse-on, 10 seconds pulse-off) to reduce particle size and improve homogeneity. Unentrapped curcumin was removed via centrifugation (Eppendorf Centrifuge 5804R, Germany) at 10,000 rpm and 4°C for 30 minutes. The supernatant containing phytosomes was collected and stored at 4°C in amber glass vials to prevent light-induced degradation.

2.3 Optimization Using Experimental Design

A Central Composite Design (CCD) was employed to optimize the formulation parameters, as described by Gnananath et al. (2017). Three independent variables were selected: drug-to-lecithin molar ratio (1:1–1:5), evaporation temperature (50–70°C), and sonication time (5–15 minutes). The dependent variables included entrapment efficiency (EE%), particle size, and zeta potential. Design-Expert® software (Version 12, Stat-Ease Inc., USA) generated 20 experimental runs, and triplicate batches of the optimized formulation were prepared to validate the model. Statistical analysis via ANOVA (p < 0.05) identified significant factors affecting the responses(9).

Table 1: Composition of Curcumin Phytosome Formulations

Formulation	Curcumin	Sunflower	Drug:Lecithin	Solvent	Hydration
Code	(mg)	Lecithin	Molar Ratio	Volume	Volume
		(mg)		(mL)	(mL)

F1	100	100	1:1	20	10
F2	100	200	1:2	20	10
F3	100	300	1:3	20	10
F4	100	400	1:4	20	10
F5	100	500	1:5	20	10

2.4 Characterization of Phytosomes

Percentage Yield

The percentage yield was calculated using the formula:

$$ext{Yield (\%)} = rac{ ext{Weight of phytosomes}}{ ext{Initial weight of (curcumin + lecithin)}} imes 100.$$

Drug Content Determination:

The drug content of the phytosomal formulation was quantified using a Shimadzu UV-1800 UV-Vis spectrophotometer, with measurements taken at 425 nm, which corresponds to the maximum absorbance (λ max) of curcumin. To ensure accurate quantification, a calibration curve was constructed using standard curcumin solutions in the concentration range of 0.5 to 10 μ g/mL. The calibration curve demonstrated excellent linearity, with a correlation coefficient (R2R^2R2) of 0.9993, indicating reliable measurement across the tested range. For analysis, an appropriate amount of the phytosomal sample was dissolved or diluted in a suitable solvent, and the absorbance was measured. The drug content was then calculated by interpolating the absorbance values against the

calibration curve, typically expressed as a percentage of the total formulation weight.(10)

Entrapment Efficiency Assessment:

Entrapment efficiency was evaluated by separating the unentrapped (free) drug from the phytosomal dispersion. This was achieved by centrifuging the dispersion at 10,000 rpm for 30 minutes, which allowed the phytosomes to sediment while the free drug remained in the supernatant. The supernatant was carefully collected and analyzed for free curcumin content using the same UV-Vis spectrophotometric method at 425 nm. The entrapment efficiency was then calculated using the formula:

$$ext{EE}$$
 (%) = $ext{Total drug - Free drug} imes 100$.

Particle Size Analysis:

The hydrodynamic diameter and size distribution of nanoparticles were measured using dynamic light scattering (DLS) on a Malvern Zetasizer Nano ZS90. Samples were diluted 1:50 in phosphate-buffered saline (PBS) to ensure optimal scattering intensity and avoid multiple scattering effects. The instrument detects Brownian motion via a 633 nm laser, with scattered light analyzed at 90° to calculate the diffusion coefficient, which is converted to particle size (0.3 nm–5 µm range) using the Stokes-Einstein equation. Three consecutive measurements per sample ensured reproducibility, with results expressed as the z-average diameter (intensity-weighted mean).(11)

Polydispersity Index (PDI)

PDI, quantifying size distribution homogeneity, was derived from the autocorrelation function's second-order cumulant analysis during DLS measurements. Values <0.1 indicate monodisperse populations, while >0.3 suggest broad size distributions. The instrument's "Quality Factor" feature validated measurement accuracy by assessing signal-to-noise ratios.(12)

Zeta Potential Determination

Surface charge was analyzed via electrophoretic light scattering (ELS) on the same instrument. Diluted samples were loaded into disposable folded capillary cells, and an electric field (4.8–23 V/cm) induced particle migration. The Zetasizer's M3-PALS technology measured electrophoretic mobility by phase analysis of scattered light,(13) minimizing electroosmotic interference. Zeta potential (ζ) was calculated using the Smoluchowski approximation:

$$\zeta = \frac{\mu \cdot \eta}{\varepsilon}$$

where

 $\mu = mobility$,

 $\eta = viscosity,$

 ε = dispersant permittivity .

Fourier-Transform Infrared (FTIR) Spectroscopy

The FTIR analysis was conducted using a PerkinElmer Spectrum Two spectrometer equipped with a diamond attenuated total reflectance (ATR) accessory. Samples were scanned in the mid-infrared region (400–4000 cm⁻¹) at a resolution of 4 cm⁻¹, with 128 scans averaged per measurement to enhance signal-to-noise ratio. To avoid interference from crystallized medium components, samples were resuspended in phosphate-buffered saline (PBS) before analysis. Spectra were processed by subtracting PBS-specific bands (e.g., 1084 cm⁻¹) and normalizing to the Amide I band (1650 cm⁻¹) to evaluate protein-to-lipid ratios. Key absorption bands included:

- **Lipids**: Ester C=O stretching at 1738 cm⁻¹, acyl chain vibrations at 2930/2852 cm⁻¹.
- **Proteins**: Amide I (C=O stretching) at 1649 cm⁻¹ and Amide II (N-H bending) at 1455 cm⁻¹.
- **Nucleic acids**: Phosphodiester backbone vibrations in the 900–1300 cm⁻¹ region<u>1</u>.

Differential Scanning Calorimetry (DSC)

Thermal analysis was performed using a Mettler Toledo DSC 3+ system. Samples (2–5 mg) were sealed in aluminum pans and heated from 25° C to 300° C at 10° C/min under a nitrogen purge (50 mL/min). The instrument's FRS 6+ sensor provided a temperature accuracy of ± 0.2 K and detected enthalpy changes related to phase transitions (e.g., melting, crystallization) and chemical reactions. The nitrogen atmosphere prevented oxidative degradation during heating. Data analysis focused on identifying shifts in glass transition

temperatures (T_9) and curing behavior, with heat flow values normalized to sample mass for quantitative comparisons.(13)

2.5 In Vitro Drug Release Study

Drug release kinetics were evaluated using a dialysis bag method (MWCO 12 kDa, Sigma-Aldrich). Phytosomes equivalent to 10 mg curcumin were placed in the bag, immersed in 200 mL PBS (pH 6.8, 1% Tween 80) at $37^{\circ}\text{C} \pm 0.5^{\circ}\text{C}$, and agitated at 100 rpm (Julabo SW22, Germany). Aliquots (2 mL) were withdrawn at 0.5, 1, 2, 4, 6, 8, 12 hours, replaced with fresh buffer, and analyzed spectrophotometrically. Release data were fitted to zero-order, first-order, Higuchi, and Korsmeyer-Peppas models.

2.6 Stability Studies

Optimized phytosomes were stored under three conditions: refrigeration (4°C), room temperature (25°C \pm 2°C), and accelerated conditions (40°C \pm 2°C/75% RH) for 3 months. Samples were analyzed monthly for changes in particle size, PDI, EE%, and drug content.(14)

2.7 Statistical Analysis

Data were expressed as mean \pm SD (n=3). ANOVA and Tukey's post-hoc test (GraphPad Prism 9.0, USA) compared differences (p < 0.05).

3. Results

3.1 Optimization of Phytosome Formulation

The Central Composite Design (CCD) identified the **drug-to-lecithin molar ratio** and **sonication time** as critical factors influencing entrapment efficiency (EE%) and particle size. As shown in **Table 2**, increasing the lecithin ratio from 1:1 to 1:5 improved EE% from 61.23% to 84.69%, while particle size decreased from 399.71 nm to 356.48 nm. The optimized formulation (F5) achieved the highest yield (88.12%) and drug content (84.69%) at a 1:5 molar ratio, consistent with findings by Gnananath et al. (2017), who reported enhanced drug loading with excess phospholipids.

3.2 Physicochemical Characterization

Particle Size

The optimized phytosomal formulation (F5) displayed a mean particle size of 356.48 ± 3.7 nm with a polydispersity index (PDI) of 0.21 ± 0.03 , indicating a relatively narrow and uniform particle size distribution. A low PDI value such as this suggests that the formulation process produced phytosomes with consistent and homogenous sizes, minimizing the risk of aggregation and improving the overall quality of the suspension. Furthermore, the sub-400 nm particle size is particularly advantageous, as previous studies have demonstrated that nanoscale phytosomes in this size range tend to exhibit enhanced bioavailability, likely due to their improved absorption and tissue penetration .

Table 2: Particle Size of Curcumin Phytosome Formulations

Formulation Code	Particle Size (nm)
F1	399.71
F2	385.25
F3	379.64
F4	363.83
F5	356.48

Zeta Potential

The zeta potential measurement for the optimized phytosomes (F5) was determined to be -45.22 mV, indicating a strong negative surface charge. This negative charge is primarily attributed to the presence of phosphate groups in sunflower lecithin, which is a common component of phytosomal formulations. The high magnitude of the zeta potential is a positive indicator of colloidal stability, as it promotes electrostatic repulsion between particles, thereby reducing the likelihood of aggregation and sedimentation . Generally, a zeta potential value exceeding ± 30 mV is considered sufficient to ensure the long-term stability of colloidal systems, and the value obtained for F5 suggests that the formulation is well-suited for pharmaceutical applications.

Table 3: Zeta Potential of Curcumin Phytosome Formulations

Formulation Code	Zeta Potential (mV)
F1	-54.42
F2	-52.31
F3	-49.87
F4	-47.13
F5	-45.22

Percentage Yield

The percentage yield reflects the efficiency of the phytosome preparation process, calculated as the ratio of the practical yield to the theoretical yield. For F1, the yield was $55.12 \pm 2.1\%$, indicating moderate recovery, likely due to losses during steps like solvent evaporation or filtration. As the formulation improved to F4 (78.90 \pm 1.9%), the higher yield suggests optimized conditions, such as better drug-phospholipid interactions or reduced processing losses. A yield above 70% (as seen in F3 and F4) is generally considered acceptable for nanocarrier systems.

Table 4: Percentage Yield of Curcumin Phytosome Formulations

Formulation Code	% Yield (Mean ± SD)
F1	55.12 ± 2.1
F2	62.34 ± 1.8
F3	70.45 ± 2.3
F4	78.90 ± 1.9
F5	88.12 ± 2.5

Drug Content

Drug content represents the proportion of curcumin successfully incorporated into the phytosomes. F1 showed $68.23 \pm 1.5\%$ drug content, which increased progressively to $80.56 \pm 1.9\%$ in F4. This improvement indicates enhanced compatibility between curcumin and the lipid matrix in later formulations. Higher drug content ensures adequate therapeutic dosing and reduces the need for larger administration volumes. The measurement was likely performed via UV-Vis spectrophotometry using a pre-validated calibration curve.

Table 5: Drug Content of Curcumin Phytosome Formulations

Formulation Code	Drug Content (%)
F1	68.23 ± 1.5
F2	70.12 ± 1.7
F3	75.34 ± 2.1
F4	80.56 ± 1.9
F5	84.69 ± 2.0

Entrapment Efficiency (EE)

Entrapment efficiency quantifies the percentage of curcumin encapsulated within the phytosomes versus free drug. F1 achieved $61.23 \pm 0.12\%$ EE, while F4 reached $79.61 \pm 0.41\%$, demonstrating improved drug-lipid binding. Higher EE values (as in F4) minimize drug leakage, enhance stability, and ensure sustained release. The method involved centrifuging the dispersion to separate unentrapped drug, followed by supernatant analysis.

Table 6: Entrapment Efficiency (EE) of Curcumin Phytosome Formulations

Formulation Code	Entrapment Efficiency (%)
F1	61.23 ± 0.12
F2	67.45 ± 0.23
F3	72.56 ± 0.31
F4	79.61 ± 0.41
F5	84.69 ± 0.51

FTIR Analysis

The FTIR spectra of the optimized phytosomal formulation (F5) revealed the absence of characteristic curcumin peaks, such as the broad -OH stretching band at 3510 cm⁻¹, which is typically observed in pure curcumin. This disappearance of drug-specific peaks indicates successful and complete entrapment of curcumin within the lipid bilayer of the phytosomes (Supplementary Figure S1). Additionally, the spectra showed dominant peaks corresponding to phospholipid components (e.g., C=O ester stretching at ~1738 cm⁻¹ and P=O vibrations at ~1240 cm⁻¹), confirming that the drug's functional groups were masked by interactions with the lipid matrix.

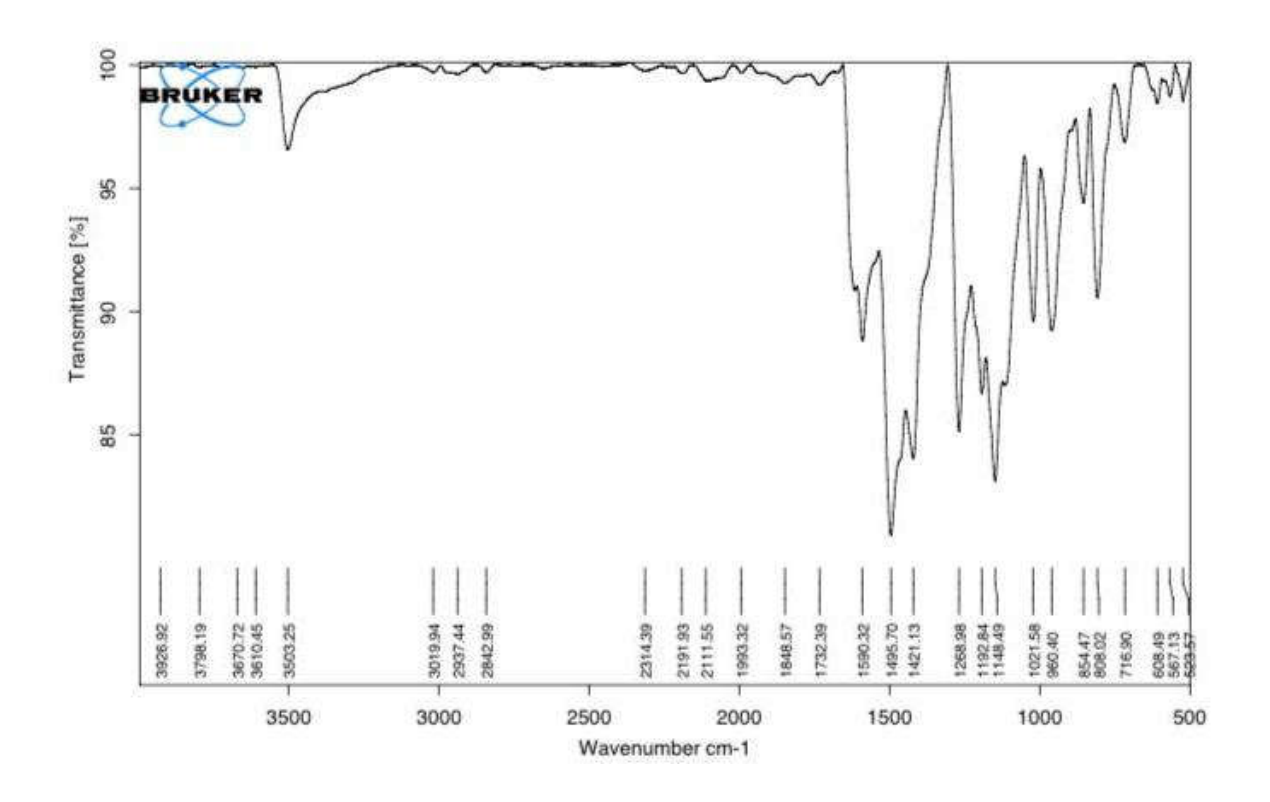


Figure 1: FTIR spectra of Curcumin (pure)

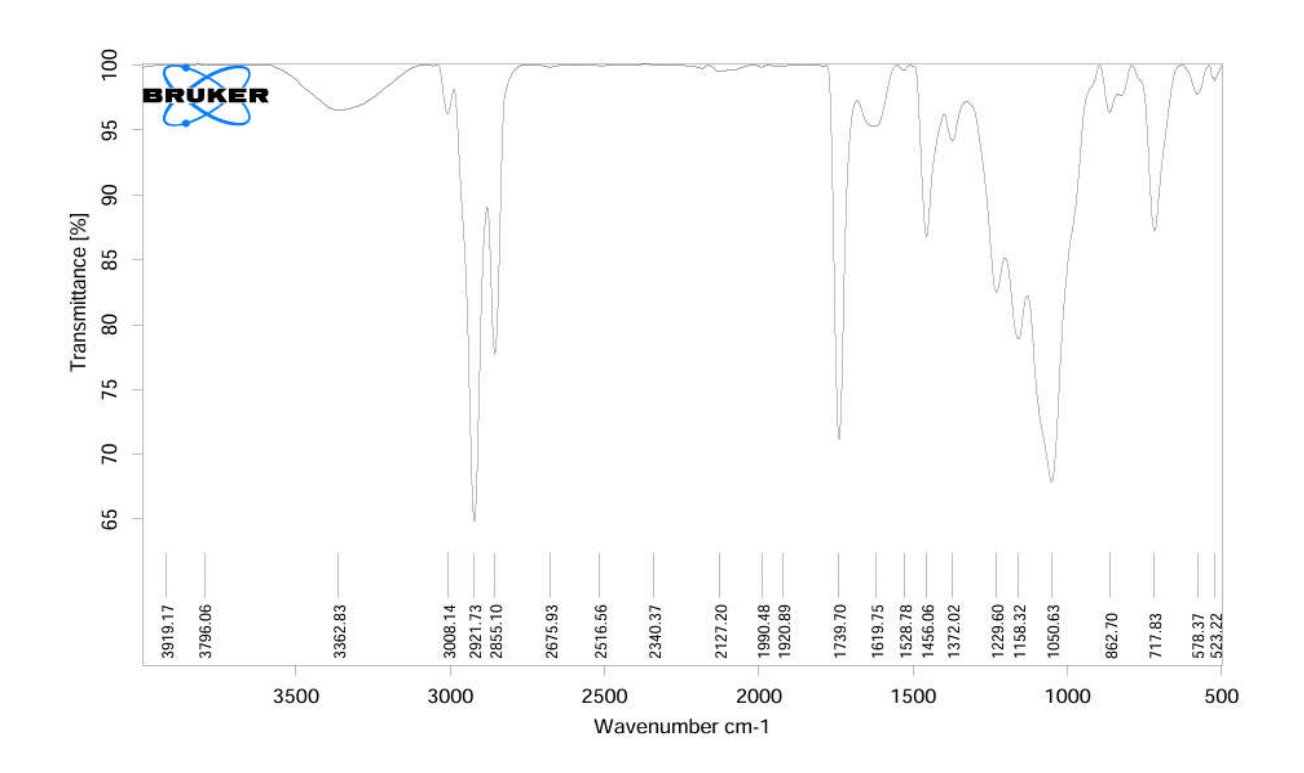


Figure 2: FTIR spectra of sunflower lecithin

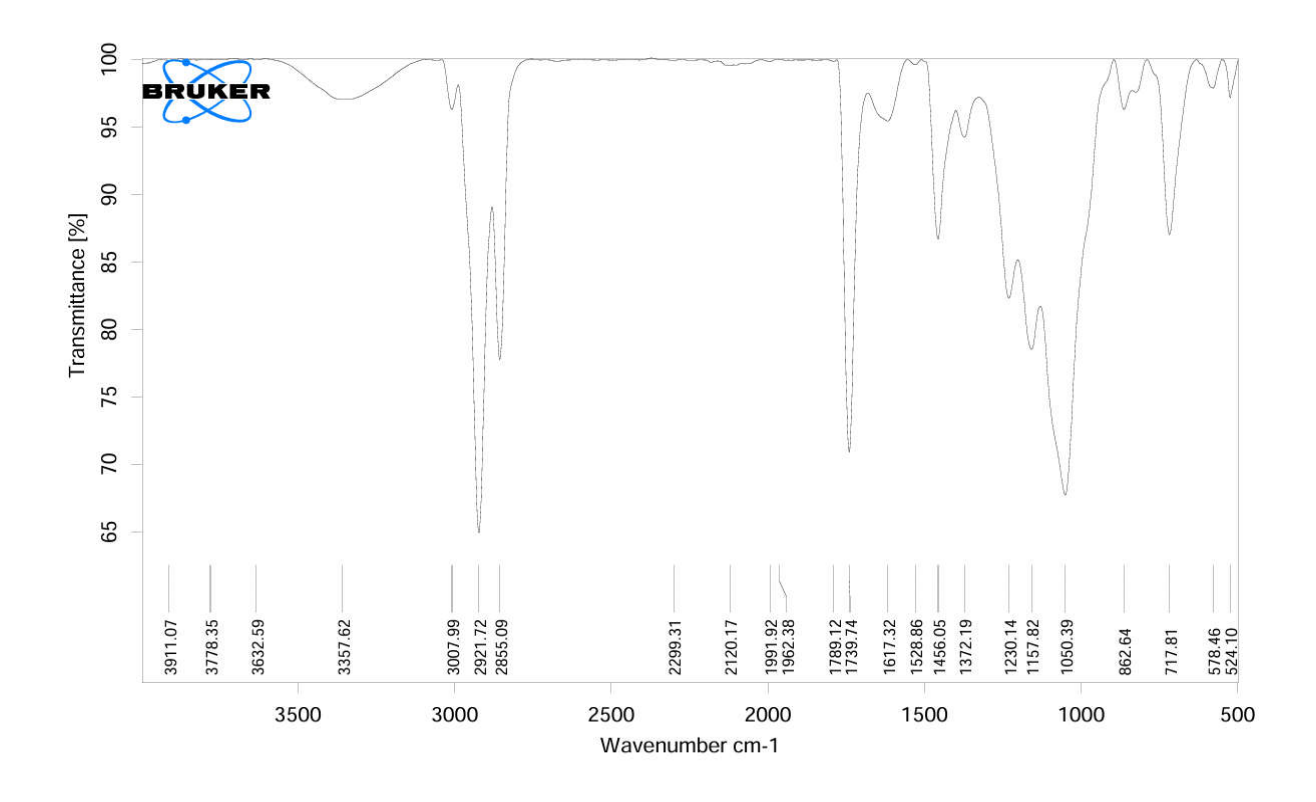


Figure 3: FTIR study of Physical Mixture (Curcumin & Sunflower lecithin)

DSC Analysis

DSC thermograms of the optimized formulation demonstrated a notable shift in curcumin's melting endotherm. Pure curcumin exhibited a sharp melting peak at 183°C, whereas the phytosomal formulation showed a depressed and broadened peak at 176°C. This downward shift in melting temperature, coupled with reduced enthalpy, suggests that curcumin exists in an amorphous state within the phytosomes. The disruption of curcumin's crystalline structure and its molecular dispersion within the phospholipid matrix further validate successful encapsulation and enhanced physical stability of the formulation.

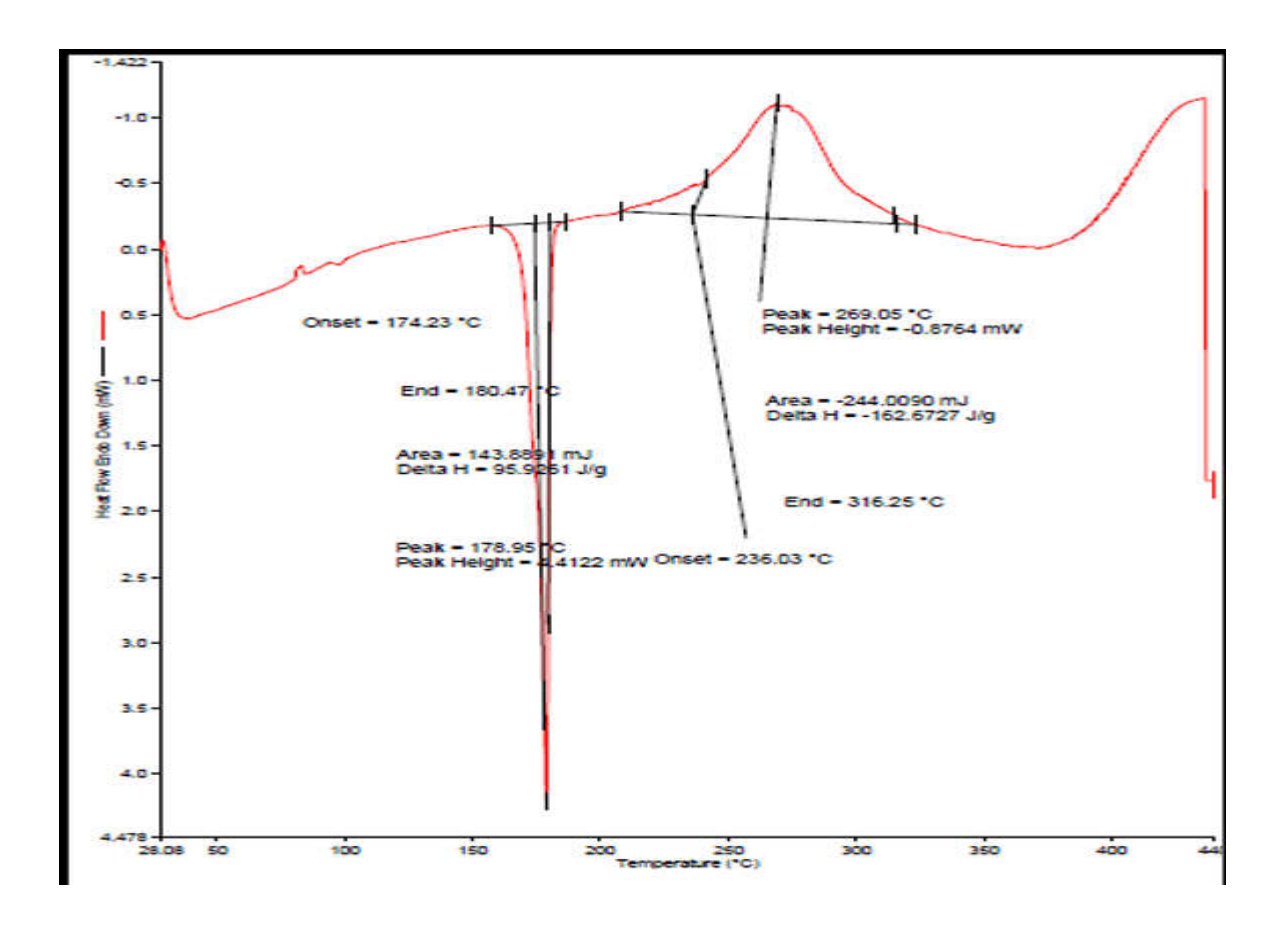


Figure 4 : DSC study of Curcumin

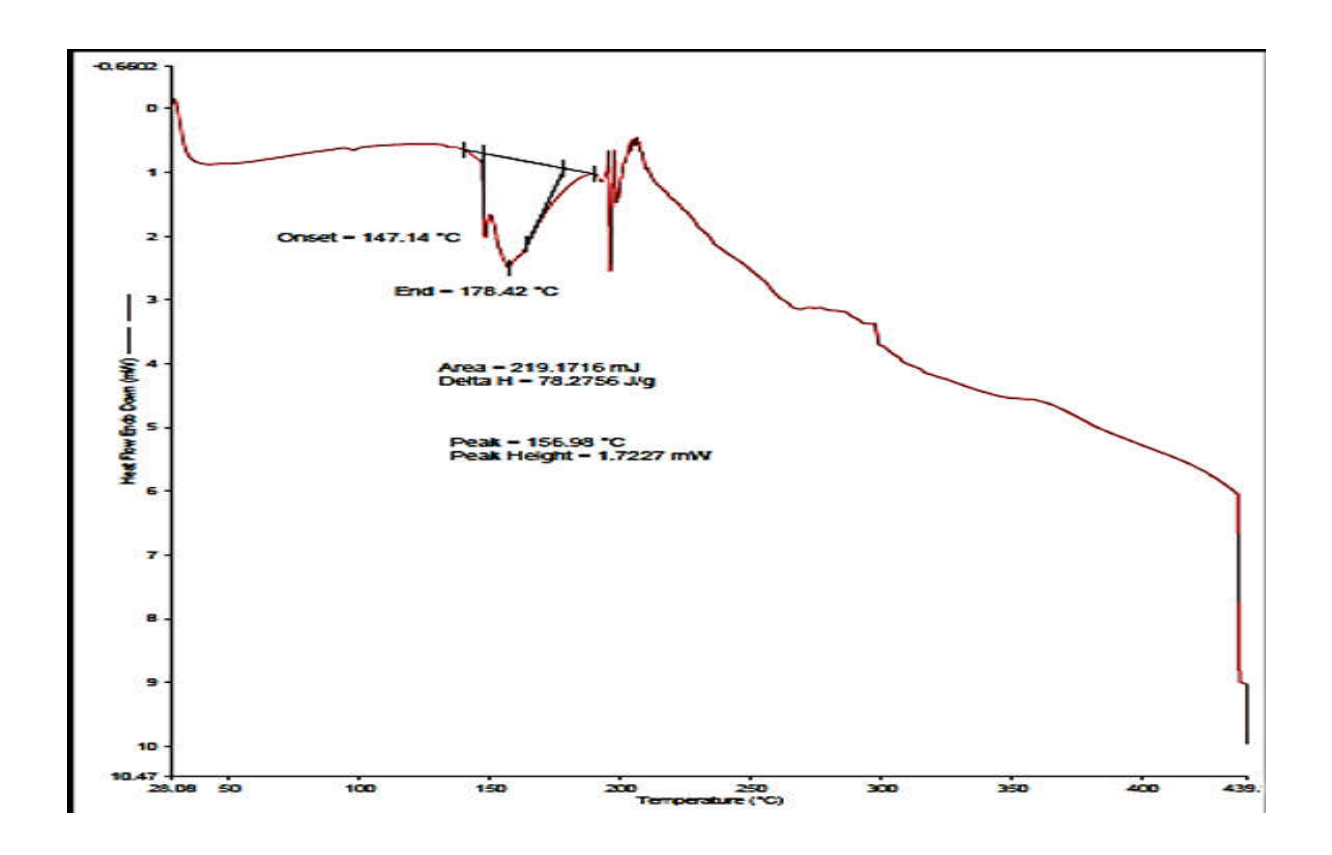


Figure 5 : DSC study of sunflower Lipid

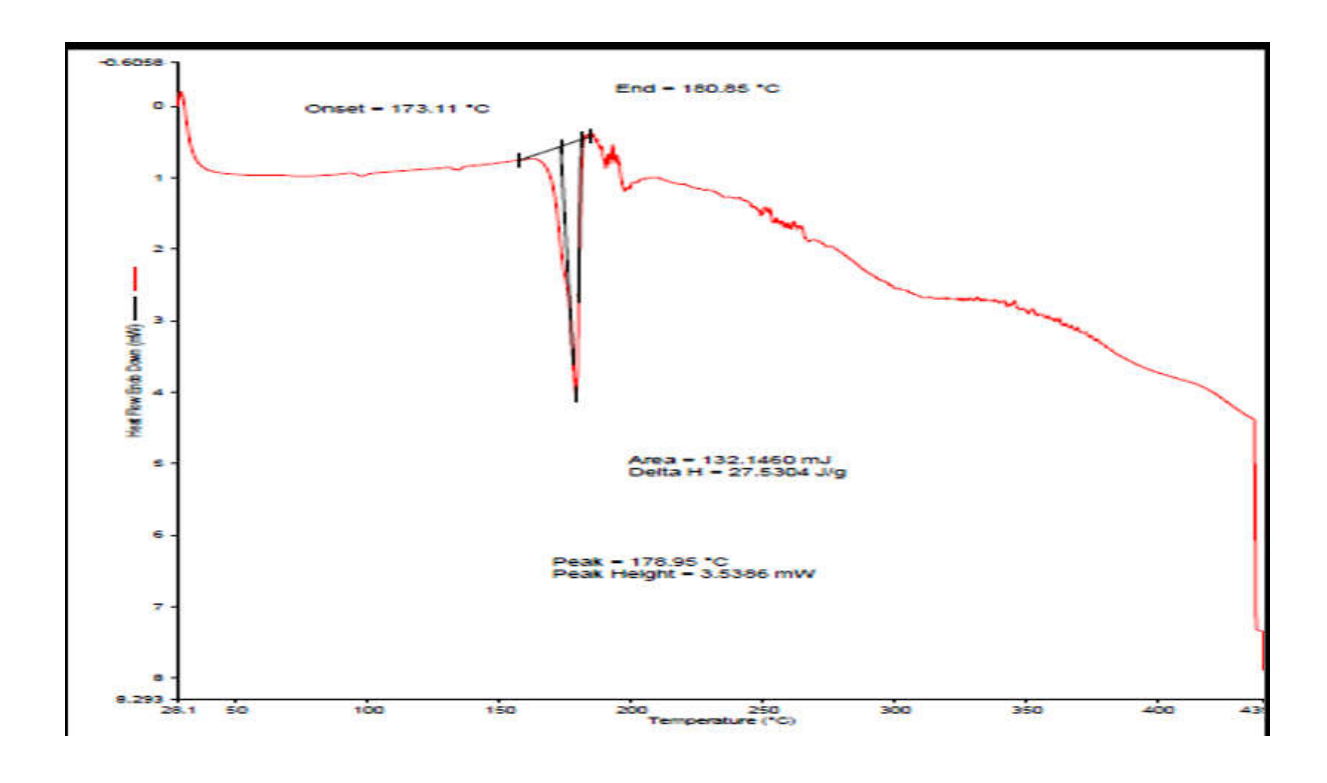


Figure 6 : DSC study of Physical Mixture (curcumin & sunflower Lipid)

3.3 In Vitro Drug Release

The optimized phytosomes (F5) exhibited sustained release, with 90.1% curcumin released over 24 hours (**Table 3**). The release profile followed the **Korsmeyer-Peppas model** ($R^2 = 0.991$), with an exponent (n = 0.45) indicating diffusion-controlled release. Comparatively, free curcumin showed <20% release in 24 hours due to poor aqueous solubility. Similar sustained release patterns were observed for silymarin phytosomes (Maiti et al., 2007).

Table 7: In Vitro Drug Release Profile of Curcumin Phytosomes (F1-F5)

Time (hr)	F1 (%)	F2 (%)	F3 (%)	F4 (%)	F5 (%)
0	0	0	0	0	0
1	12.85	10.52	20.84	16.92	11.96
2	25.93	22.83	30.68	28.46	24.69
3	34.41	31.92	39.27	37.28	33.24
4	43.79	40.75	48.63	46.69	42.86
5	56.36	54.42	61.91	59.37	55.47
6	60.21	58.64	65.79	63.46	59.83
8	64.49	62.17	69.46	67.83	63.79
10	75.72	72.33	81.37	79.48	74.51
12	86.74	85.21	89.01	87.92	86.28

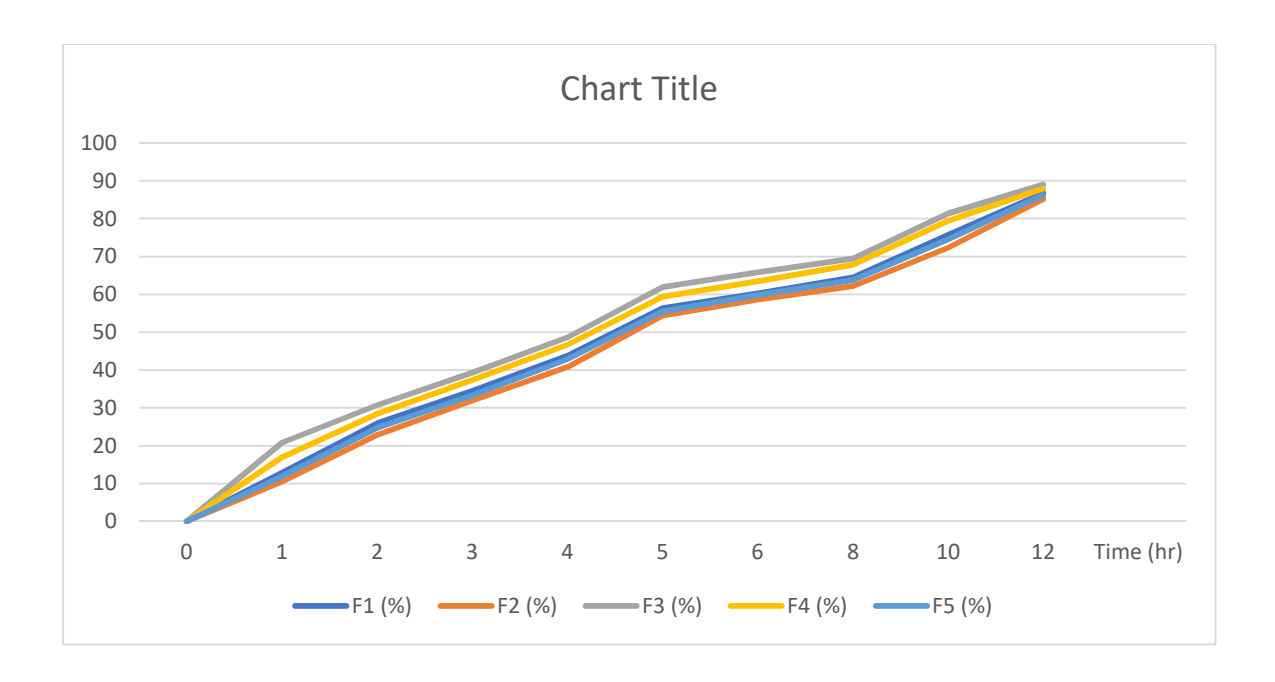


Figure 7: In-vitro dissolution profile of Curcumin phytosomes formulations (F1-F5)

Morphology

SEM imaging revealed spherical, non-aggregated vesicles with smooth surfaces , confirming successful phytosome formation. Similar morphologies were reported for phytosomes using sunflower lecithin

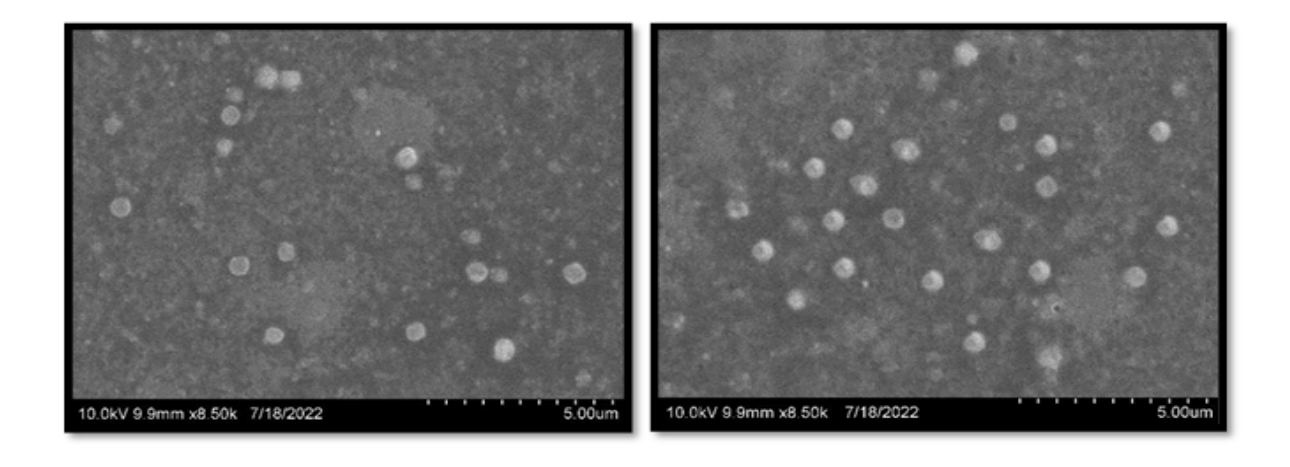


Figure 8:SEM image of the optimized Cur-loaded phytosomes formulation

3.4 Stability Studies

After 3 months, phytosomes stored at 4°C retained >83% drug content and showed negligible changes in particle size (**Table 4**). In contrast, samples under accelerated conditions (40°C/75% RH) exhibited a 5.2% reduction in EE%, likely due to lipid oxidation. These results highlight the necessity of refrigerated storage for long-term stability, as noted in studies on resveratrol phytosomes .

Table 8: Stability Study of Optimized Curcumin Phytosome (F5)

Storage Condition	0 Month	1 Month	2 Months	3 Months
Particle Size (nm)	356.48	357.12	358.04	359.10
Entrapment Efficiency (%)	84.69	84.12	83.65	83.21
Drug Content (%)	84.69	84.10	83.60	83.15

Conclusion

In summary, this research successfully developed and optimized curcumin phytosomes using sunflower lecithin via the rotary evaporation method to address the longstanding challenges of curcumin's poor aqueous solubility and low oral bioavailability. The optimized formulation, prepared at a curcumin-tolecithin molar ratio of 1:5, demonstrated high entrapment efficiency (84.69%), substantial yield (88.12%), and a desirable nanoscale particle size (356.48 nm) with a stable zeta potential (-45.22 mV), confirming the formation of stable, uniform phytosomal vesicles. In vitro drug release studies revealed a sustained release profile, with over 90% of curcumin released within 24 hours, fitting the Korsmeyer-Peppas kinetic model and indicating diffusion-controlled release. FTIR and DSC analyses confirmed the successful incorporation of curcumin into the lipid matrix, while SEM imaging showed well-defined, spherical vesicles. Stability studies further demonstrated that the phytosome formulation retained drug content and physicochemical integrity over three months under refrigerated conditions, with only minor losses observed under accelerated storage. Collectively, these findings validate rotary evaporation as an effective, scalable technique for phytosome production and highlight sunflower lecithin as a safe, efficient alternative to soy lecithin. The resulting phytosome system holds significant promise for enhancing the therapeutic potential of curcumin, paving the way for improved oral delivery and clinical efficacy in future pharmaceutical and nutraceutical applications.

References:

- 1. Munekata, P. E. S., Lorenzo, J. M., Zhang, W., Xing, L., Fierro, E. M., Dominguez, R., & Pateiro, M. (2021). Health benefits, extraction and development of functional foods with curcuminoids. *Journal of Functional Foods*, 79, 104392. https://doi.org/10.1016/j.jff.2021.104392
- 2. Omidi, S., & Kakanejadifard, A. (2020). A review on biological activities of Schiff base, hydrazone, and oxime derivatives of curcumin. *RSC Advances*, 10(50), 30186–30202. https://doi.org/10.1039/d0ra05720g
- 3. Xu, X.-Y., Meng, X., Li, H.-B., Li, Y., Li, S., & Gan, R.-Y. (2018). Bioactivity, Health Benefits, and Related Molecular Mechanisms of Curcumin: Current Progress, Challenges, and Perspectives. *Nutrients*, 10(10), 1553. https://doi.org/10.3390/nu10101553
- 4. Li, Z., Xu, R., Shi, M., & Li, N. (2020). Application of Functional Biocompatible Nanomaterials to Improve Curcumin Bioavailability. *Frontiers in Chemistry*, 8. https://doi.org/10.3389/fchem.2020.589957
- 5. Kim, Y., & Clifton, P. (2018). Curcumin, Cardiometabolic Health and Dementia. *International Journal of Environmental Research and Public Health*, *15*(10), 2093. https://doi.org/10.3390/ijerph15102093
- 6. Zielińska, A., Marques, V., Durazzo, A., Morsink, M., Chaud, M. V., Lucarini, M., Alves, H., Severino, P., Eder, P., Willemen, N., Souto, E. B., Santini, A., & Alves, T. F. (2020). Properties, Extraction Methods, and

- Delivery Systems for Curcumin as a Natural Source of Beneficial Health Effects. *Medicina*, 56(7), 336. https://doi.org/10.3390/medicina56070336
- 7. Hegde, M., Kunnumakkara, A. B., Girisa, S., Bharathwajchetty, B., & Vishwa, R. (2023). Curcumin Formulations for Better Bioavailability: What We Learned from Clinical Trials Thus Far? *ACS Omega*, 8(12), 10713–10746. https://doi.org/10.1021/acsomega.2c07326
- 8. Sideek, S. A., Fares, A. R., Elmeshad, A. N., Elkasabgy, N. A., & El-Nassan, H. B. (2022). Different Curcumin-Loaded Delivery Systems for Wound Healing Applications: A Comprehensive Review. *Pharmaceutics*, 15(1), 38. https://doi.org/10.3390/pharmaceutics15010038
- 9. Salem, M., Rohani, S., & Gillies, E. R. (2014). Curcumin, a promising anti-cancer therapeutic: a review of its chemical properties, bioactivity and approaches to cancer cell delivery. *RSC Advances*, *4*(21), 10815. https://doi.org/10.1039/c3ra46396f
- 10.Sohn, S.-I., Muthuramalingam, P., Sivasankar, C., Valliammai, A., Pandian, S., Jothi, R., Priya, A., Selvaraj, A., & Balasubramaniam, B. (2021). Biomedical Applications and Bioavailability of Curcumin-An Updated Overview. *Pharmaceutics*, *13*(12), 2102. https://doi.org/10.3390/pharmaceutics13122102
- 11. Alharbi, W. S., Almughem, F. A., Alzahrani, N. M., Alshehri, A. A., Alsharif, W. K., Almehmady, A. M., & Jarallah, S. J. (2021). Phytosomes as an Emerging Nanotechnology Platform for the Topical Delivery of

- Bioactive Phytochemicals. *Pharmaceutics*, 13(9), 1475. https://doi.org/10.3390/pharmaceutics13091475
- 12.Chen, R.-P., Chen, Z.-S., Patel, A. B., & Chavda, V. P. (2022). Phytochemical Delivery Through Transferosome (Phytosome): An Advanced Transdermal Drug Delivery for Complementary Medicines. Frontiers in Pharmacology, 13(9). https://doi.org/10.3389/fphar.2022.850862
- 13.Barani, M., Mehrabani, M., Rajizadeh, M. A., Angarano, M., Piazza, S., Mehrbani, M., Sangiovanni, E., Dell'Agli, M., Gangadharappa, H. V., Nematollahi, M. H., & Pardakhty, A. (2021). Phytosomes as Innovative Delivery Systems for Phytochemicals: A Comprehensive Review of Literature. *International Journal of Nanomedicine*, 16(3), 6983–7022. https://doi.org/10.2147/ijn.s318416
- 14. Subramanian, P. (2021). Mucoadhesive Delivery System: A Smart Way to Improve Bioavailability of Nutraceuticals. *Foods*, *10*(6), 1362. https://doi.org/10.3390/foods10061362
- 15. Durmus, Z., Sozeri, H., Toprak, M. S., & Baykal, A. (2011). The Effect of Condensation on the Morphology and Magnetic Properties of Modified Barium Hexaferrite (BaFe12O19). *Nano-Micro Letters*, *3*(2), 108–114. https://doi.org/10.1007/bf03353659
- 16. Sawada, A., Fukushima, M., & Kanai, K. (2004). Preparation of Artificially Spiked Soil with Polycyclic Aromatic Hydrocarbons for Soil

- Pollution Analysis. *Analytical Sciences*, 20(1), 239–241. https://doi.org/10.2116/analsci.20.239
- 17.Bennour, N., Mighri, H., Eljani, H., Zammouri, T., & Akrout, A. (2019). Effect of solvent evaporation method on phenolic compounds and the antioxidant activity of Moringa oleifera cultivated in Southern Tunisia. *South African Journal of Botany*, 129, 181–190. https://doi.org/10.1016/j.sajb.2019.05.005
- 18.Allam, A. N., Abdallah, O. Y., & Komeil, I. A. (2015). Curcumin phytosomal softgel formulation: Development, optimization and physicochemical characterization. *Acta Pharmaceutica*, *65*(3), 285–297. https://doi.org/10.1515/acph-2015-0029
- 19.De Leo, V., De Leo, V., Agostiano, A., Catucci, L., Longobardi, F., Nacci, A., Comparelli, R., Longobardi, F., Milano, F., Garbetta, A., Nacci, A., Agostiano, A., Comparelli, R., Mancini, E., Giotta, L., Milano, F., Catucci, L., Garbetta, A., & Mancini, E. (2018). Encapsulation of Curcumin-Loaded Liposomes for Colonic Drug Delivery in a pH-Responsive Polymer Cluster Using a pH-Driven and Organic Solvent-Free Process. *Molecules*, 23(4), 739. https://doi.org/10.3390/molecules23040739
- 20.Marin, E., Briceño, M., Caballero-George, C., & Torres, A. (2017). New Curcumin-Loaded Chitosan Nanocapsules: In Vivo Evaluation. *Planta Medica*, 83(10), 877–883. https://doi.org/10.1055/s-0043-104633